Reactions of Phosphorus-Containing Species of Importance in the Catalytic Recombination of H + OH: Quantum Chemical and Kinetic Studies†

John C. Mackie,* George B. Bacskay, and Naomi L. Haworth

School of Chemistry, University of Sydney, NSW 2006, Australia

Received: March 5, 2002; In Final Form: April 29, 2002

Four reactions of potential importance in the catalytic recombination of H + OH in the presence of phosphorus compounds have been studied by ab initio quantum chemical and RRKM methods. These are the reactions $HOPO + OH \rightarrow (HO)_2PO \rightarrow H_2O + PO_2$ (3), $HOPO + H \rightarrow P(OH)_2 \rightarrow H_2O + PO$ (4), $(HO)_2PO + H \rightarrow P(OH)_3 \rightarrow H_2O + HOPO$ (5), and $HOPO_2 + H \rightarrow (HO)_2PO \rightarrow H_2O + PO_2$ (6). Each of these reactions takes place by recombination with small (<5 kcal mol^{-1}) or no barrier to form an adduct. The subsequent decomposition of the adducts occurs by the elimination of H_2O through four-centered transition states. The thermochemistry of these reactions including the heats of formation of each of the adducts and the appropriate transition states was computed by the Gaussian G3X and G3X2 methods. Overall rate coefficients for each of these reactions at temperatures from 1000 to 2000 K and at pressures between 1 and 10 000 Torr were computed by the MultiWell code developed by Barker (Barker, J. R. *Int. J. Chem. Kinet.* **2001**, *33*, 232). For each reaction, there is very little stabilization of the adduct; hence the reactions are essentially pressure-independent. For reaction 6, its overall rate coefficient for the addition/decomposition mechanism greatly exceeds that previously derived for an abstraction transition state (Haworth, N. L.; Bacskay, G. B.; Mackie, J. C. *J. Phys. Chem. A* **2002**, *106*, 1533−1541**)**.

Introduction

In a recent contribution[1] we reported the results of quantum chemical calculations on certain key reactions in the recombination of H and OH catalyzed by the phosphorus oxides and acids, PO_2, HOPO, and $HOPO_2$, namely the reactions

$$H + PO_2 (+M) \rightarrow HOPO (+M) \quad (1a)$$

$$H + HOPO \rightarrow H_2 + PO_2 \quad (1b)$$

$$OH + H_2 \rightarrow H_2O + H \quad (1c)$$

and

$$OH + PO_2 (+M) \rightarrow HOPO_2 (+M) \quad (2a)$$

$$H + HOPO_2 \rightarrow H_2O + PO_2 \quad (2b)$$

These are the reactions proposed by Twarowski[2,3] to account for the catalytic recombination observed when oxidation products of PH_3 are present in the combustion products of hydrogen in the presence of oxygen. Twarowski[4] proposed a kinetic model of 175 reactions of 24 species, 17 of which contain P compounds. A serious limitation of the model has been the lack of reliable thermochemical and kinetic data, especially for the phosphorus species. Recently Korobeinichev and co-workers[5] revisited this model with rate coefficients for reactions of certain of the phosphorus-containing species optimized to measured species profiles. Substantial differences existed between the rate coefficients adopted by Korobeinichev et al.[5] and Twarowski for the key reactions 1a,b and 2a,b which we resolved through ab initio computations of thermochemical and kinetic parameters.

From an examination of the two sets of reactions 1a−c and 2a,b, it can be seen that both lead to the recombination of H and OH to produce H_2O. This catalytic behavior should also be of importance in the application of phosphorus compounds as potential flame suppressants.[6] However, one can postulate other possible reactions between the important flame gas radicals H and OH and phosphorus oxides and acids which might be of comparable or even greater importance than (1a,b) and (2a,b). The above cycles involve abstraction routes (1b) and (2b) to the recombination products. Phosphorus oxides and acids should also be capable of undergoing reactions of addition with OH or H and subsequent decomposition of the adducts to recombination products. Possible addition/decomposition reactions of importance include

$$HOPO + OH \rightarrow (HO)_2PO \rightarrow H_2O + PO_2 \quad (3)$$

$$HOPO + H \rightarrow P(OH)_2 \rightarrow H_2O + PO \quad (4)$$

$$(HO)_2PO + H \rightarrow P(OH)_3 \rightarrow H_2O + HOPO \quad (5)$$

$$HOPO_2 + H \rightarrow (HO)_2PO \rightarrow H_2O + PO_2 \quad (6)$$

Some of these reactions might produce competing pathways or additional catalytic cycles to (1a−c) and (2a,b), and in the case of reaction 6, it provides an alternative mechanism to that of abstraction (2b). Thus, the purpose of the present article is to provide reliable ab initio thermochemistry and rate coefficients for reactions 3−6.

Theory and Computational Methods

Each of the reactions 3−6 takes place by chemical activation

$$R^{\bullet} + XPO \underset{k_{uni}}{\overset{k_{rec}}{\rightleftharpoons}} XPOR^* \rightarrow H_2O + YPO \quad (7)$$

† Part of the special issue "R. Stephen Berry Festschrift".

* Corresponding author. E-mail: j.mackie@chem.usyd.edu.au.

10.1021/jp025727j CCC: $22.00
Published on Web 08/13/2002

TABLE 1: Lennard-Jones and Energy Transfer Parameters

param	value
	$P(OH)_2$
σ	5.0 Å
ϵ/k_B	200 K
	$(HO)_2PO$ and $P(OH)_3$
σ	5.5 Å
ϵ/k_B	250 K
	Argon
σ	3.66 Å
ϵ/k_B	179 K
	Energy Transfer[a]
γ	0.7
$\alpha(E)$	$43.5 + 0.0042E$ cm^{-1}

[a] Used in the collision step-size distribution function $f_d(E,E') = \exp\{-|((E' - E)/\alpha(E'))|^\gamma\}$, $E' > E$. See ref 7.

where R• is either H or OH, X is HO, $(HO)_2$, or HOO, and YPO represents either HOPO, PO_2, or PO. XPOR* represents the vibrationally excited species formed on recombination. The chemically activated species can either react via the reverse of reaction 7 or undergo unimolecular decomposition to the final products H_2O + YPO. All of the studied reactions have qualitatively similar potential energy surfaces along the reaction coordinate, as will be shown in the next section. In each reaction the adduct XPOR* corresponds to a local minimum on the potential energy surface; i.e., it is an exothermic process. The subsequent barriers to decomposition to the products H_2O + YPO are relatively small.

Our model for the recombination kinetics assumes that the vibrationally excited adduct XPOR* formed at an energy E will undergo the reverse reaction at an energy-specific rate coefficient $k(E)$. The limiting high-pressure rate coefficient, $k_{uni,\infty}$, is given by

$$k_{uni,\infty} = \frac{1}{q(T)}\int_{E_0}^{\infty} k(E)\rho(E)\exp(-E/k_BT)\,dE \qquad (8)$$

where $q(T)$ is the adduct's internal partition function calculated at translational temperature T, $\rho(E)$ is the density of states, and k_B is the Boltzmann constant. The lower limit for integration is the critical energy E_0. The recombination rate coefficient in the high-pressure limit, $k_{rec,\infty}$, is obtained from $k_{uni,\infty}$ by detailed balance using the equilibrium constant $K_c(T)$ as

$$k_{rec,\infty} = k_{uni,\infty}/K_c(T) \qquad (9)$$

Finally, the overall pressure-dependent rate coefficient for overall decomposition to products H_2O + YPO is given by

$$k_{overall} = f_{prods}k_{rec,\infty} \qquad (10)$$

To evaluate $\rho(E)$, $k_{uni,\infty}$, and f, the fraction of species (reactants, stabilized adduct, or products) produced at quasi-steady state, we have employed the MultiWell suite of programs recently developed by Barker[7,8] to solve the internal master equation with densities of states calculated by an exact count method. Collisional energy transfer parameters used in the calculations are given in Table 1. For the XPOR phosphorus-containing adducts, there are no literature values of the Lennard-Jones parameters, σ, and ϵ/k_B, so we have estimated these from known parameters of comparably sized molecules. The calculations are not very sensitive to moderate variations in these parameters.

Stationary states on the potential energy surfaces for each of the reactions 3−6 were determined by quantum chemical calculations. For stable species and for well-defined transition states, i.e., first-order saddle points, the Gaussian 3X (G3X) method of Pople and co-workers[9] and the related G3X2 technique[1] have been employed. In these approaches the energies of the atomic and molecular species of interest are obtained via quadratic configuration interaction (QCISD(T)) calculations in a split valence + polarization functions basis (6-31G(d)), which are then corrected by MP4, MP2, and SCF estimates of the energy changes with systematic enlargement of the basis sets and by empirical higher level corrections. G3X differs from the original G3 method[10] in that the geometries and vibrational frequencies in a G3X (and G3X2) calculation are determined by density functional theory (DFT), specifically by B3LYP/6-31G(2df,p) computations, and in the case of systems with second or higher row elements an additional basis set correction is applied. For such systems the largest basis is the G3Xlarge set; in G3X the energetic contribution of going beyond the G3large basis is evaluated at the SCF level, while in G3X2 the corresponding contribution is obtained by MP2, in an attempt to take advantage of the greater correlating capability of the G3Xlarge basis. Open shell systems are generally treated by the unrestricted versions of the above approaches, except in the case of PO and PO_2, for which a variant of the G3(RAD) approach of Radom and co-workers[11−13] was used, where the unrestricted Hartree−Fock based computations are replaced by their restricted open shell analogues.

For reactions 3 and 5, at correlated levels of theory, such as density functional theory (DFT) and complete active space second-order perturbation theory (CASPT2), the recombinations were found to be barrierless with no saddle point to define the transition state. For these reactions, therefore, the transition state geometries were determined by variational transition state theory (VTST), whereby the rate coefficients $k_{uni,\infty}$ were evaluated along the intrinsic reaction coordinate, the transition state having the geometry where the rate coefficient is at a minimum, as described in our earlier publication.[1] In the current work the individual points on the reaction coordinate were computed by DFT, using the B3LYP functional in conjunction with Dunning's cc-pVDZ basis set.[14,15] Further details of the calculations will be given in the next section.

The G3X and G3X2 calculations were carried out using the Gaussian98 programs.[16] Complete active space self-consistent field (CASSCF) and CASPT2 test calculations were performed using DALTON[17] and MOLCAS,[18] to carry out CASSCF geometry optimizations and correlated energy calculations, respectively. The computations were performed on DEC alpha 600/5/333 and COMPAQ XP1000/500 workstations of the Theoretical Chemistry group at the University of Sydney.

Results and Discussion

Quantum Chemistry. The heats of formation (at 0 K), rotational constants, and vibrational frequencies of the transition states, as found by the application of the G3X method, are given in Table 2. Similar details are provided in Table 3 for each of the adducts: $(HO)_2P$; $(HO)_2PO$; $(HO)_3P$. The geometries of all these species, determined at the B3LYP/6-31G(2df,p) level of theory, are given in Table S1 of the Supporting Information. (The geometries, rotational constants, and frequencies for HOPO, $HOPO_2$, PO, and PO_2 are given in our earlier study.[1]) The G3X and G3X2 total energies as well as heats of formation at 298 K of all species relevant to this work are listed in Table 4. Although in this work only the G3X energies are used in the computation of rate coefficients, the G3X2 results are included for completeness. While the differences between the G3X and

TABLE 2: Computed Heats of Formation, Rotational Constants, and Vibrational Frequencies of Transition States[a]

reacn no. and reactants	transition state tsa[b]				transition state tsb[b]			
	name	$\Delta_f H^0_0$/ kcal mol^{-1}	rotational consts/cm^{-1}	vib freq/cm^{-1}	name	$\Delta_f H^0_0$/ kcal mol^{-1}	rotational consts/cm^{-1}	vib freq/cm^{-1}
(3) HOPO + OH	ts1	−100.2	0.2963, 0.1172, 0.0977	18i, 45, 155, 297, 383, 515, 566, 844, 946, 1230, 3552, 3681	ts2	−114.5	0.3324, 0.2155, 0.1451	1477i, 242, 387, 512, 542, 689, 846, 982, 1243, 1310, 1954, 3703
(4) HOPO + H	ts3	−52.2	0.9531, 0.2906, 0.2312	1127i, 203, 378, 446, 516, 831, 949, 1144, 3694	ts4	−48.7	0.6338, 0.3483, 0.2288	1434i, 483, 530, 684, 804, 1034, 1342, 1901, 3716
(5) $(HO)_2PO$ + H	ts5	−102.2	0.2600, 0.2322, 0.1421	174i, 82, 131, 207, 243, 354, 376, 444, 805, 851, 1013, 1025, 1212, 3714, 3764	ts6	−148.7	0.2834, 0.2024, 0.1522	1409i, 220, 341, 451, 510, 561, 697, 757, 846, 969, 1078, 1333, 1901, 3682, 3725
(6) $HOPO_2$ + H	ts7	−103.5	0.3006, 0.2546, 0.1430	1020i, 180, 279, 381, 430, 472,502, 869, 1021, 1133, 1388, 3732	ts2	−114.5	as above	as above

[a] Computed at 1000 K for variational transition states ts1 and ts5. [b] Refer to Figure 1.

G3X2 heats of formation are typically 2−3 kcal mol^{-1}, there is a large degree of cancellation when reaction energies are computed. This makes the thermochemistry and rate coefficients studied in this work quite insensitive to the choice of G3 type method.

As indicated in the previous section, VTST was used to locate the geometries of two transition states, ts1 and ts5, which correspond to the HOPO (^{1}A′) + OH ($^2\Pi$) and $(HO)_2PO$ (^{2}A) + H (^{2}S) recombination reactions, respectively. In the former case, as the reaction involves making a P−O(H) σ-bond while breaking the PO π-bond of HOPO, one would expect to find a saddle point to describe the transition state. Such a saddle point, corresponding to a tight transition state geometry, was located when using the CASSCF method. However, on recalculation of the energy at a correlated level of theory, either by CASPT2 or DFT, the CASSCF transition state was found to lie ∼29 kcal mol^{-1} *lower* in energy than the reactants HOPO + OH. As no saddle point could be found by DFT, we used VTST to locate the transition state. The reaction coordinate was approximated by a minimum energy path on the potential energy surface, where each point corresponds to fixed, relatively large values of the P−O(H) distance with all other geometric parameters fully optimized at the B3LYP/cc-pVDZ level of theory. The frequencies of the vibrational modes orthogonal to the reaction coordinate were computed by projecting out the contamination in the Hessian by the nonzero gradient.[20] The effect of such projection was found to be quite small, since at large P−O(H) distances the gradient with respect to the reaction coordinate is very small and the (quadratic) coupling between reaction coordinate and the vibrational modes is very weak. The minimum in the computed rate coefficients was located at a P−O(H) distance of ∼3.0 Å (as shown in the structure of ts1 in Table S1 of the Supporting Information). The same VTST approach was used to locate the transition state ts5 associated with the radical recombination reaction $(HO)_2PO$ + H, where the OH distance was determined to be ∼2.6 Å. The final geometries (optimized with respect to all parameters other than the critical PO and OH distances previously determined), projected frequencies, and energies for these transition states were redetermined at the B3LYP/6-31G(2df,p) level of theory. In the case of the energy, the B3LYP energy difference between reactants and transition state in each of these systems was scaled by the ratio of the G3X/B3LYP reaction energy and corrected for basis set superposition effects by the Boys−Bernardi counterpoise method.[21] Using the energy differences as described above, reasonable estimates of the total G3X energies of ts1 and ts5 could be provided.

The resulting schematic G3X potential energy surfaces are shown in Figure 1a−d. As discussed above, the HOPO + OH recombination reaction 3 (see Figure 1a) is found to be barrierless. The standard heat of reaction (at 298 K) is computed to be −54.6 kcal mol^{-1}. The dissociation of the resulting adduct, viz. $(HO)_2PO \rightarrow H_2O + PO_2$, is endothermic, with a reaction enthalpy of 31.4 kcal mol^{-1} and an enthalpy of activation of 38.8 kcal mol^{-1}. By contrast, the HOPO + H recombination reaction 4 (see Figure 1b) has a small barrier of 7.4 kcal mol^{-1}, while the standard heat of reaction is −30.2 kcal mol^{-1}. The thermochemistry for the subsequent elimination of water is very similar to that in reaction 3, the reaction enthalpy being 23.2 kcal mol^{-1} while the enthalpy of activation is 33.6 kcal mol^{-1}. The $(HO)_2PO$ + H recombination reaction 5 (see Figure 1c) is also barrierless, but in this instance the resulting adduct, viz. $P(OH)_3$, appears to be much more stable, since the heat of this reaction is −82.1 kcal mol^{-1}. The dissociation of this species

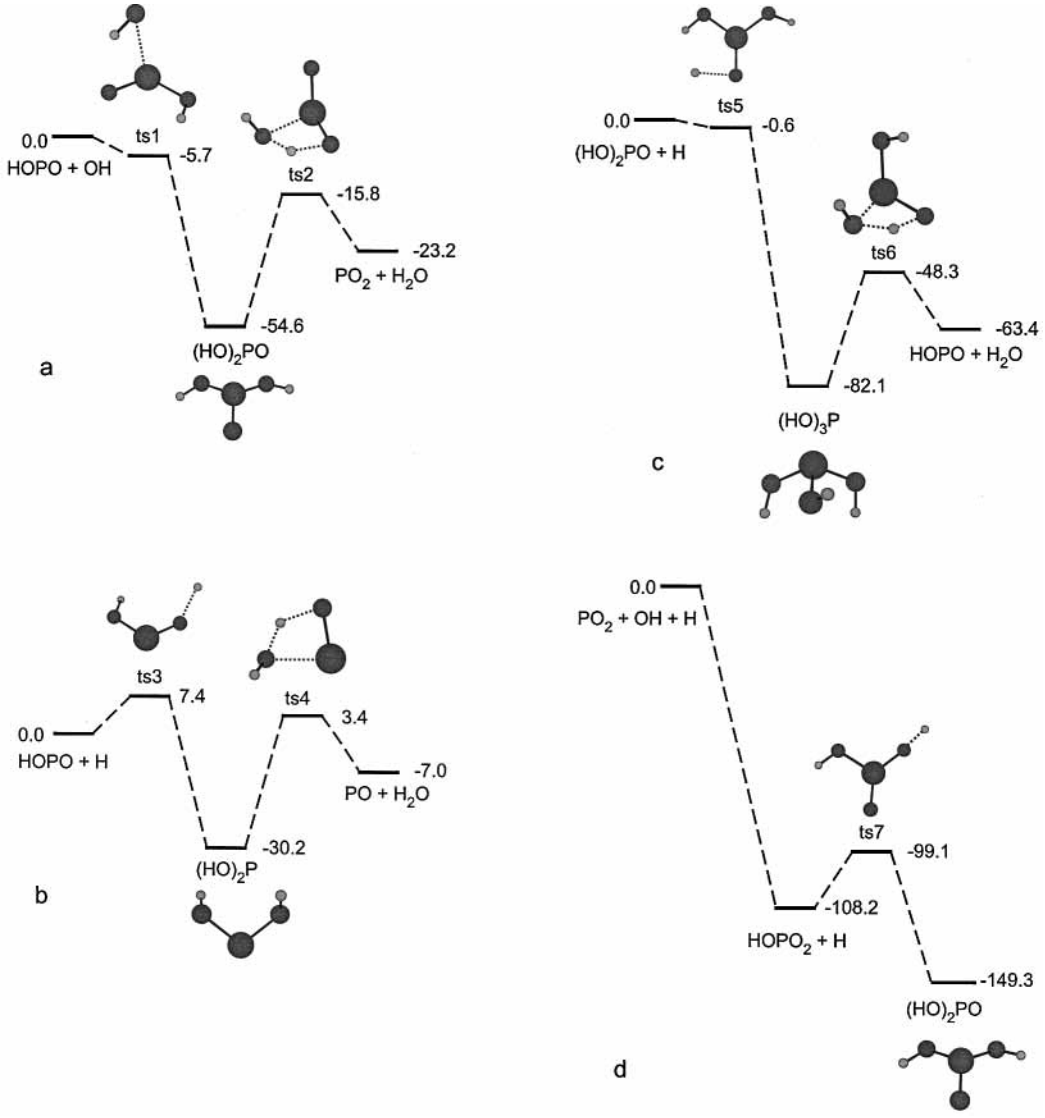

Figure 1. Schematic potential energy surfaces for reactions 3−6. Stationary points correspond to relative enthalpies at 298 K computed at the G3X level of theory.

TABLE 3: Heats of Formation, Rotational Constants, and Vibrational Frequencies of Adducts

adduct	$\Delta_f H^0_0$/kcal mol^{-1}	rotational consts/cm^{-1}	vib freq/cm^{-1}
$(HO)_2PO$	−153.8	0.2857, 0.2597, 0.1469	117, 277, 350, 388, 455, 810, 840, 1009, 1022, 3769, 3771
$P(OH)_2$	−86.4	0.8487, 0.2916, 0.2228	131, 274, 407, 789, 804, 926, 973, 3714, 3716
$P(OH)_3$	−183.1	0.2573, 0.2347, 0.1535	158, 215, 300, 388, 427, 451, 773, 806, 833, 965, 994, 1067, 3699, 3714, 3789

TABLE 4: Total Energies and Heats of Formation at 298 K Computed at G3X and G3X2 Levels of Theory

	Eo(0 K)/*Eh*		$\Delta_f H^\circ_{298}$/kcal mol^{-1}			*Eo*(0 K)/*Eh*		$\Delta_f H^\circ_{298}$/kcal mol^{-1}	
species	G3X	G3X2	G3X	G3X2	species	G3X	G3X2	G3X	G3X2
PO ($^2\Sigma$) ($C_{\infty v}$)	−416.406 53[a]	−416.414 74[a]	−7.7[a]	−9.0[a]	ts3 (^{1}A) (C_1)	−492.733 80	−492.739 83	−50.8	−52.8
PO_2 (^{2}A$_1$) (C_{2v})	−491.635 37[a]	−491.644 68[a]	−67.6[a]	−69.6[a]	ts4 (^{1}A) (C_1)	−492.739 36	−492.745 04	−54.8	−56.6
HOPO-*cis* (^{1}A′) (C_s)	−492.246 08	−492.252 23	−110.3	−112.3	ts5 (^{1}A) (C_1)	−568.528 43[b]		−104.9	
$HOPO_2$ (^{1}A′) (C_s)	−567.462 32	−567.470 03	−167.4	−170.5	ts6 (^{1}A) (C_1)	−568.602 71	−568.609 37	−152.6	−155.0
H_2O (^{1}A$_1$) (C_{2v})	−76.383 23	−76.383 23	−57.5	−57.5	ts7 (^{1}A) (C_1)	−567.947 37	−567.954 92	−106.2	−109.1
OH ($^2\Sigma$) (C_v)	−75.696 07	−75.696 07	8.4	8.4	P	−341.116 99	−341.119 84	75.6[c]	
$(HO)_2P$ (^{2}A) (C_1)	−492.793 83	−492.799 49	−88.3	−90.1		−341.140 14[a]	−341.14624[a]		
$(HO)_2PO$ (^{2}A) (C_1)	−568.027 52	−568.034 20	−156.4	−158.8	O	−75.032 24	−75.032 24	59.6[c]	
$(HO)_3P$ (^{1}A) (C_1)	−568.657 43	−568.664 11	−186.4	−188.8		−75.040 29[a]	−75.040 29[a]		
ts1 (^{1}A) (C_1)	−576.950 08[b]		−107.5		H	−0.500 97	−0.500 97	52.1[c]	52.1
ts2 (^{1}A) (C_1)	−567.964 92	−567.971 79	−117.6	−120.2					

[a] G3X(RAD) and G3 · 2(RAD) values. [b] Obtained indirectly as described in text. [c] Experimental value.[19]

to HOPO + H_2O is very similar to the water elimination step in reactions 3 and 4, with a reaction enthalpy of 18.7 kcal mol^{-1} and an enthalpy of activation of 33.8 kcal mol^{-1}. Since the barriers to water elimination are fairly low, they are not expected to have a substantial effect on the overall kinetics unless substantial stabilization of the adducts occurs. Finally, the

TABLE 5: Pressure-Dependent Rate Coefficients for Overall Decomposition

		$10^{-12}k_{overall}$/cm^3 mol^{-1} s^{-1}						
reacn	*T*/K	10 000 Torr	1000 Torr	760 Torr	532 Torr	100 Torr	10 Torr	1 Torr
(3) HOPO + OH → H_2O + PO_2	1000	1.48	1.64	1.70	1.71	1.70	1.64	1.68
	2000	3.09	3.27	3.11	3.15	3.13	3.26	3.07
(4) HOPO + H → H_2O + PO	1000	0.123	0.157	0.167	0.157	0.157	0.153	0.158
	2000	1.56	1.30	1.44	1.45	1.38	1.44	1.25
(5) $(HO)_2PO$ + H → H_2O + HOPO	1000	17.3	17.5	17.5	17.5	17.3	17.5	17.5
	2000	49.6	49.2	48.8	46.7	48.5	48.5	48.4
(6) $HOPO_2$ + H → H_2O + PO_2	1000	0.0594	0.0977	0.0950	0.0973	0.100	0.0993	0.0999
	2000	2.18	2.12	2.09	2.19	2.06	2.14	2.16

TABLE 6: Computed Overall Rate Coefficients: Arrhenius and Modified Arrhenius Fit Parameters[a]

	Arrhenius		modified Arrhenius		
reacn	log *A*	E_a	log *A*	n	E_a
(3) HOPO + OH → H_2O + PO_2	12.78	2.6	13.57	−0.219	3.2
(4) HOPO + H → H_2O + PO	13.10	8.8	12.50	0.166	8.3
(5) $(HO)_2PO$ + H → H_2O + HOPO	14.14	4.0	18.92	−1.334	7.7
(6) $HOPO_2$ + H → H_2O + PO_2	13.66	12.2	13.03	0.176	11.8

[a] Units for *A*, cm^3 mol^{-1} s^{-1}; units for E_a, kcal mol^{-1}.

recombination reaction $HOPO_2$ + H (eq 6) (see Figure 1d) is found to have a small barrier, corresponding to an enthalpy of activation of 9.1 kcal mol^{-1}, while the standard heat of reaction is found to be −41.1 kcal mol^{-1}. The reaction of PO_2 with OH yielding $HOPO_2$ was studied in detail in our previous work. It was found to be a barrierless reaction, and as indicated in Figure 1d, it is highly exothermic.

Kinetic Parameters. For the reactions 3−6 chemical activation simulations were carried out over the temperature range of 1000−2000 K and pressures from 1 to 10 000 Torr using the MultiWell code. The temperature range spans the ranges studied by Korobeinichev et al.[5] and Twarowski.[2,3] These pressures include that studied by Twarowski (532 Torr) and 760 Torr. Simulations were carried out to steady state in the concentrations of stabilized adduct, initial reactants, and final products. Pressure-dependent overall rate coefficients for product formation were calculated by means of eqs 9 and 10. These rate coefficients at the lowest and highest temperatures of the studied range are tabulated as a function of pressure in Table 5.

As may be seen from Table 5, apart from the highest pressure studied (10 000 Torr), there is very little stabilization of the adducts; hence, the rate coefficients for overall reactions show little or no variation with pressure. Simple averaging of the rate coefficients obtained at pressures from 1 to 1000 Torr lead to Arrhenius plots which are very nearly linear although the temperature variation of the individual rate coefficients can be expressed slightly more accurately by the modified Arrhenius form $k_{overall} = AT^n \exp(-E_a/RT)$. Both Arrhenius and modified Arrhenius parameters for reactions 3−6 are given in Table 6.

From Tables 5 and 6 we see that the values of $k_{overall}$ for all of the reactions 3−6 are comparable with or exceed the abstraction rate coefficients we derived in our earlier work[1] for reactions 1b and 2b. Thus, in future modeling of the catalytic recombination of H + OH by phosphorus oxides and acids, reactions 3−6 should be included. Furthermore, reaction 6 involves the same reactants and final products as reaction 2b. The rate coefficient we have now derived for the addition and decomposition route is nearly 3 orders of magnitude larger at 1000 K than the abstraction rate coefficient and at 2000 K is more than 1 order of magnitude larger than the latter. Clearly, this reaction takes place via an energized adduct rather than through an abstraction transition state.

In their recent experimental and modeling study of the destruction of organophosphorus compounds and flames, Korobeinichev et al.[5] measured the [$HOPO_2$] concentration and the [HOPO]/[PO] ratio in the flame by mass spectrometry. As a consequence, to match these measured concentrations they made some arbitrary changes in rate coefficients of reactions 3, 4, and 6, lowering the values from those originally postulated by Twarowski[2−4] by between 1 and 2 orders of magnitude. Our calculated rate coefficients for (3), (4), and (6) are larger than those adopted by Korobeinichev et al.[5] by approximately this same order of magnitude and thus agree quite well with the original Twarowski values. In addition, Korobeinichev et al.[5] observed a peak at 81 amu in their mass spectra which they attributed to the species $(HO)_2PO$ which they considered to be a significant intermediate. In their modeling they included an estimated value of the rate coefficient for the reaction $(HO)_2PO$ + H → H_2O + HOPO (eq 5) of 1×10^{12} cm^3 mol^{-1} s^{-1}, a value which is between 1 and 2 orders of magnitude less than our calculated value given in Table 6.

At 1000 K and at a pressure of 10 000 Torr, there is a small amount of stabilized adduct $(HO)_2PO$ arising from reaction 3. Computed fractional populations at steady state under these conditions are $f\{(HO)_2PO\} = 0.122$, $f\{H_2O + PO_2\} = 0.698$, and $f\{HOPO + OH\} = 0.180$. If the $(HO)_2PO$ adduct is sufficiently long-lived, reactions 3 and 5 may be considered to constitute a catalytic pathway for H + OH recombination with HOPO acting as the catalyst. However, this would be a minor catalytic recombination pathway operating only at high pressures and low temperatures.

Conclusion

We have studied several reactions of importance in the recombination of H + OH catalyzed by the phosphorus oxides and acids PO, PO_2, HOPO, and $HOPO_2$. These reactions take place by addition and subsequent decomposition of the adduct which eliminates H_2O via four-center transition states of low barrier. These reactions are essentially pressure-independent and are much faster than the alternative mechanism of abstraction. The reactions lead to rapid equilibration of the phosphorus oxides and acids and might lead to more rapid recombination of H and OH than previously considered.

Acknowledgment. N.L.H. gratefully acknowledges the award of an Australian Postgraduate Research Scholarship.

Supporting Information Available: Table S1, containing geometries of adducts and transition states. This material is available free of charge via the Internet at http://pubs.acs.org.

References and Notes

(1) Haworth, N. L.; Bacskay, G. B.; Mackie, J. C. *J. Phys. Chem. A* **2002**, *106*, 1533−1541.
(2) Twarowski, A. *Combust. Flame* **1993**, *94*, 91.
(3) Twarowski, A. *Combust. Flame* **1993**, *94*, 341.
(4) Twarowski, A. *Combust. Flame* **1995**, *102*, 41.

(5) Korobeinichev, O. P.; Ilyin, S. B.; Bolshova, T. A.; Shvartsberg, V. M.; Chernov, A. A. *Combust. Flame* **2000**, *121*, 593.

(6) Macdonald, M. A.; Jayaweera, T. M.; Fisher, E. M.; Gouldrin, F. C. *Combust. Flame* **2001**, *125*, 668.

(7) Barker, J. R. *Int. J. Chem. Kinet.* **2001**, *33*, 232.

(8) Barker, J. R. *MultiWell Software Version 1.2.0*; http://aoss.engin.umich.edu/multiwell/, Ann Arbor, MI, 2002.

(9) Curtiss, L. A.; Redfern, P. C.; Raghavachari, K.; Pople, J. A. *J. Chem. Phys*. **2001**, *114*, 108.

(10) Curtiss, L. A.; Raghavachari, K.; Redfern, P. C.; Rassolov, V.; Pople, J. A. *J. Chem. Phys*. **1998**, *109*, 7764.

(11) Henry, D. J.; Radom, L. In *Theoretical Thermochemistry*; Cioslowski, J.; Kluwer: Dordrecht, The Netherlands, 2001.

(12) Mayer, P. M.; Parkinson, C. J.; Smith, D. M.; Radom, L. *J. Chem. Phys*. **1998**, *108*, 604.

(13) Parkinson, C. J.; Mayer, P. M.; Radom, L. *J. Chem. Soc., Perkin Trans. 2* **1999**, 2305.

(14) Dunning, T. H. *J. Chem. Phys.* **1987**, *90*, 1007.

(15) Woon, D. E.; Dunning, T. H. *J. Chem. Phys.* **1990**, *98*, 1358.

(16) Frisch, M. J.; Trucks, G.; W.; Schlegel, H. B.; Scuseria, G. E.; Robb, M. A.; Cheeseman, J. R.; Zakrzewski, V. G.; Montgomery, J. A.; Stratmann, R. E.; Burant, J. C.; Dapprich, S.; Millam, J. M.; Daniels, A. D.; Kudin, K. N.; Strain, M. C.; Farkas, O.; Tomasi, J.; Barone, V.; Cossi, M.; Cammi, R.; Mennucci, B.; Pomelli, C.; Adamo, C.; Clifford, S.; Ochterski, J.; Petersson, G. A.; Ayala, P. Y.; Cui, Q.; Morokuma, K.; Malik, D. K.; Rabuk, A. D.; Raghavachari, K.; Foresman, J. B.; Cioslowski, J.; Ortiz, J. V.; Stefanov, B. B.; Lui, G.; Liashenko, A.; Piskorz, P.; Komaromi, I.; Gomperts, R.; Martin, R. L.; Fox, D. J.; Keith, T.; Al-Laham, M. A.; Peng, C. Y.; Nanayakkara, A.; Gonzalez, C.; Challacombe, M.; Gill, P. M. W.; Johnson, B. G.; Chen, W.; Wong, M. W.; Andres, J. L.; Head-Gordon, M.; Replogle E. S.; Pople, J. A. *Gaussian 98*, revision A.7; Gaussian, Inc.: Pittsburgh, PA, 1998.

(17) DALTON, an ab initio electronic structure program, Release 1.0 1997, written by T. Helgaker, H. J. Aa. Jensen, P. Joergensen, J. Olsen, K. Ruud, H. Aagren, T. Andersen, K. L. Bak, V. Bakken, O. Christiansen, P. Dahle, E. K. Dalskov, T. Enevoldsen, B. Fernandez, H. Heiberg, H. Hettema, D. Jonsson, S. Kirpekar, R. Kobayashi, H. Koch, K. V. Mikkelsen, P. Norman, M. J. Packer, T. Saue, P. R. Taylor, and O. Vahtras.

(18) Andersson, K.; Blomberg, M. R. A.; Fülscher, M. P.; Karlström, G.; Lindh, R.; Malmqvist, P.-Å.; Neogrády, P.; Olsen, J.; Roos, B. O.; Sadlej, A. J.; Schültz, M.; Seijo, L.; Serrano-Andrés, L.; Siegbahn, P. E. M.; Widmark, P.-O. *MOLCAS Version 4*; Lund University: Lund, Sweden, 1997.

(19) Chase, M. W. Jr. *NIST-JANAF Thermochemical Tables*, 4th ed.; *J. Phys. Chem. Ref. Data*. **1998**, *Monograph 9*, 1.

(20) Baboul, A. G.; Schlegel, H. B. *J. Chem. Phys*. **1997**, *107*, 9413.

(21) Boys, S. F.; Bernardi, F. *Mol. Phys*. **1970**, *19*, 553.